J Neurophysiol 101: 2984–2994, 2009.
First published March 25, 2009; doi:10.1152/jn.90713.2008.

Contributions of Primate Prefrontal and Posterior Parietal Cortices to Length and Numerosity Representation

Oana Tudusciuc and Andreas Nieder
Department of Animal Physiology, Institute of Zoology, University of Tübingen, Tübingen, Germany

Submitted 24 June 2008; accepted in final form 16 March 2009

Tudusciuc O, Nieder A. Contributions of primate prefrontal and posterior parietal cortices to length and numerosity representation. *J Neurophysiol* 101: 2984–2994, 2009. First published March 25, 2009; doi:10.1152/jn.90713.2008. The ability to understand and manipulate quantities ensures the survival of animals and humans alike. The frontoparietal network in primates has been implicated in representing, along with other cognitive abilities, abstract quantity. The respective roles of the prefrontal and parietal areas and the way continuous quantities, as opposed to discrete ones, are represented in this network, however, are unknown. We investigated this issue by simultaneously analyzing recorded single-unit activity in the prefrontal cortex (PFC) and the fundus of the intraparietal sulcus (IPS) of two macaque monkeys while they were engaged in delayed match-to-sample tasks discriminating line length and numerosity. In both areas, we found anatomically intermingled neurons encoding either length, numerosity, or both types of quantities. Even though different sets of neurons coded these quantities, the representation of length and numerosity was similar within the IPS and PFC. Both length and numerosity were coded by tuning functions peaking at the preferred quantity, thus supporting a labeled-line code for continuous and discrete quantity. A comparison of the response characteristics between parietal and frontal areas revealed a larger proportion of IPS neurons representing each quantity type in the early sample phase, in addition to shorter response latencies to quantity for IPS neurons. Moreover, IPS neurons discriminated quantities during the sample phase better than PFC neurons, as quantified by the receiver operating characteristic area. In the memory period, the discharge properties of PFC and IPS neurons were comparable. These single-cell results are in good agreement with functional imaging data from humans and support the notion that representations of continuous and discrete quantities share a frontoparietal substrate, with IPS neurons constituting the putative entry stage of the processing hierarchy.

INTRODUCTION

Behavioral studies in humans show that number, space, and time interfere with each other (Henik and Tzelgov 1982; Walsh 2003). These psychophysical findings imply that different types of magnitudes are represented in common brain networks. Brain studies in both human and nonhuman primates using a variety of methodological approaches have evidenced that both the prefrontal and the posterior parietal cortices play cardinal roles in magnitude processing (Dehaene et al. 2003, 2004; Walsh 2003). However, where and how single neurons encode different types of abstract quantity and what the respective contributions of cortical areas are questions that remain largely unanswered.

In the numerical domain, single-unit recordings in behaving monkeys have implicated the prefrontal and posterior parietal cortices in processing abstract numerosity (Nieder and Miller 2004; Nieder et al. 2002, 2006) and functional imaging studies in humans have emphasized the role of the frontoparietal network in the representation of number and arithmetic operations in humans (Dehaene et al. 1999; Eger et al. 2003; Piazza et al. 2007; Simon et al. 2002). Both the prefrontal and the posterior parietal cortices of the macaque have been studied intensively in the context of spatial information processing in a variety of cognitive protocols (Bisley and Goldberg 2003; Colby and Goldberg 1999; Rainer et al. 1998; Rao et al. 1996; Wilson et al. 1993) and neuroimaging studies of spatial cognition in humans have identified putatively homolog parietal and prefrontal areas (Astafiev et al. 2003; Medendorp et al. 2003; Merriam et al. 2003; Orban et al. 2004).

Recently it has also been demonstrated that time-interval judgments in macaques activate regions in both the prefrontal (Genovesio et al. 2006) and the posterior parietal (Leon and Shadlen 2003) cortices. In a more extensive investigation of the brain activity related to time-interval judgment, functional imaging data in monkeys (Onoe et al. 2001) show that the frontoparietal cortical regional cerebral blood flow covaries with time-interval judgment. This suggests a frontoparietal network of neurons engaged in time processing, again also supported in humans based on imaging studies (Buhusi and Meck 2005; Macar and Vidal 2002; Macar et al. 2002, 2004). Together, converging evidence in human and nonhuman primates points to the frontoparietal network as a likely candidate for the representation of temporal, spatial, and numerical quantity (Buhusi and Meck 2005; Nieder 2005; Walsh 2003).

In many of these studies, special types of magnitude have been investigated in isolation. To evaluate whether different magnitude representations really access a comparable neural substrate, more than a single quantity should ideally be studied in the same individual. In an elegant functional imaging study, Pinel and colleagues (2004) investigated the neuronal correlates of the behavioral interference between numbers and space. The authors measured the brain activity of human subjects engaged in a quantity-comparison task in which they compared two Arabic symbols, but based on different comparison criteria from block to block (number value, physical symbol size, and luminosity). They found that the physical size and the numerical size comparison activity overlaps in one region in the horizontal part of the intraparietal sulcus (Pinel et al. 2004). These results—along with other functional imaging (Castelli et al. 2006; Fias et al. 2003; Kaufmann et al. 2005), transcranial magnetic stimulation (Cohen Kadosh et al. 2007; Gobel et al. 2001), and neuropsychological (Cohen Kadosh et al. 2007; Rossetti et al. 1998; Zorzi et al. 2002) studies in humans—suggest that anatomical vicinity in the cortex might be responsible for behavioral interference phenomena between numerical and spatial quantities (Hubbard et al. 2005).

Address for reprint requests and other correspondence: A. Nieder, Department of Animal Physiology, Institute of Zoology, University of Tübingen, Auf der Morgenstelle 28, 72076 Tübingen, Germany (E-mail: andreas.nieder@uni-tuebingen.de).

In a previous work, we showed that the posterior parietal cortex is involved in the representation of both continuous and discrete quantities (Tudusciuc and Nieder 2007). By analyzing single-unit activity in the depth of the intraparietal sulcus of two monkeys performing a quantity-discrimination task based on line length and numerosity, we found two populations of neurons, one tuned to continuous quantities, the other to discrete ones, which were functionally overlapping, meaning that 20% of these cells responded to both continuous and discrete quantities. We could thus confirm the representation of spatial quantity in the posterior parietal cortex and characterize the relationship between the discrete and continuous quantities at the level of single cells.

Yet, whether continuous quantities are represented in the prefrontal cortex and, if so, how such representations of continuous magnitudes are related to the representation of discrete quantities in the prefrontal cortex so far remain open questions. Furthermore, the respective contributions of the posterior parietal and prefrontal neurons in the processing of continuous quantities are unknown. Using simultaneous multisite, multielectrode recordings, here we compare the specific roles of each area in the representation of these two different instances of magnitude at the level of single neurons.

METHODS

Stimuli

Numerosity stimuli were black dots (diameter range 0.5 to 1.1° of visual angle) randomly placed on a circular gray background (6° of visual angle in diameter) presented in the center of the monitor. The size, total area, and position of the dots varied randomly from trial to trial. Line-length stimuli consisted in one horizontal black line displayed at random locations on a gray background circle (6° diameter, centered on the screen). The lengths of the lines were multiples of 0.85° of visual angle (line 1: 0.85°; line 2: 1.7°; line 3: 2.55°; line 4: 3.4°; line 5: 4.25°; line 6: 5.1°). The thickness of the lines varied randomly across trials from 0.06 to 0.36° of visual angle. To prevent the memorization of visual patterns, the monkeys were tested with different displays for each trial and the displays were generated randomly each day, by shuffling relevant item features (e.g., position and size). In each trial, sample and test displays never showed the identical images. To ensure that the monkeys solved the task based on the relevant quantitative information (length or numerosity, respectively), other covarying features of the stimuli were controlled in separate sets of stimuli, called control stimuli, and the positions of the dots and lines were greatly varied. For the numerosity protocol we generated control stimuli equating for the total area and thus also luminance and contrast, total circumference, the density, and the geometrical configuration of the dots in a display. For the length protocol, we created control stimuli in which the total area of the lines was kept constant across the four sample lengths. Trials were randomized and balanced across all relevant features (line length vs. numerosity, match vs. nonmatch, standard vs. control, etc.).

Behavioral task

We trained rhesus monkeys (*Macaca mulatta*) in a delayed match-to-sample (DMS) task (Nieder et al. 2002) to discriminate the two types of quantity, randomly alternating within each session. In the *length protocol* (Fig. 1*A*), the length of a line (out of four different lengths) needed to be discriminated (continuous-spatial quantity). In the *numerosity protocol* (Fig. 1*B*), the number of (one to four) items in multiple-dot displays (discrete-numerical quantity) was the relevant stimulus dimension. A trial started when the monkey grabbed a lever and fixed its gaze on a fixation spot that appeared in the middle of the screen. The monkeys maintained their gaze within 1.75° of the central fixation spot (measured using an infrared eye-monitoring system; Iscan). While maintaining fixation, monkeys viewed a sample stimulus (800 ms) followed by a delay (1,000 ms), then were allowed to freely move their eyes to evaluate test stimulus (1,200 ms). To receive a reward, the monkeys had to release a lever if the test had the same length as the sample in the length protocol or the same numerosity as the sample in the numerosity protocol. The monkeys had to maintain the lever if the first test was showing a different length in the length protocol or a different set size in the numerosity protocol, respectively. After the reward (or the wrong response) the monkey again had to grab the lever to start another trial. Each session consisted of length and numerosity trials, in random order, with equal probability. The stimuli were generated anew for each recording session, using a custom-made MatLab program designed to randomly assign the position and thickness of the standard length stimuli and the position, area, and distance to the other dots for each dot in the standard numerosity displays. For the controlled stimuli, all but the controlled parameter were randomly assigned. During each session, the monkeys were presented with standard and control stimuli, pseudorandomly, with equal probability.

Recordings

Recordings were made from one left and one right hemisphere in the depth (9–13 mm below the cortical surface) of the intraparietal sulcus (IPS) and in the prefrontal cortex (PFC) of two rhesus monkeys while they performed the DMS task. For each session, arrays of four to eight electrodes were simultaneously in the IPS and the PFC, for a total of 12 to 16 electrodes per session. The electrodes were lowered in pairs, each pair being attached to a custom-made mechanical microdrive with a precision of three complete turns per millimeter. The IPS was chosen because it contains the highest proportion of

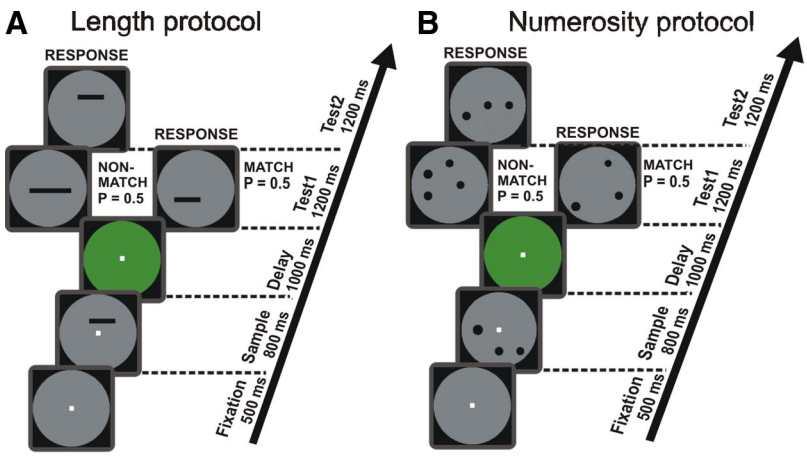

FIG. 1. Delayed match-to-sample protocol. *A*: length protocol. A trial started when the monkey grasped a lever and maintained fixation. The monkey had to release the lever if the lines in the sample and test displays had the same length and continue holding it if they did not ($P = 0.5$). Nonmatch stimuli consisted of lines that were longer or shorter than the sample line, respectively. *B*: numerosity protocol. Task conditions were identical to the length protocol, but here the monkeys had to match the number of items in the sample and test displays. The physical appearance of the displays varied widely for the same numerosities. Nonmatch stimuli showed lower or higher numerosities than the sample numerosity, respectively.

visual numerosity-selective neurons in the parietal cortex (Nieder and Miller 2004) and is specifically activated by quantity information in humans (Eger et al. 2003, Piazza et al. 2004). The PFC was also associated with a high proportion of numerosity-selective neurons (Nieder et al. 2002). All procedures were done in accordance with the guidelines for animal experimentation approved by the Regierungspräsidium Tübingen, Germany. Recordings were localized using stereotaxic reconstructions from magnetic resonance images. Neurons were randomly sampled, with no attempt to select them based on task selectivity. Both monkeys are still engaged in quantity-discrimination studies. Separation of single-unit waveforms was performed off-line, applying mainly principal component analysis (Plexon Systems).

Sensitivity to quantity stimuli

Sample activity was derived from an 800-ms interval after stimulus onset shifted by a cell's individual response latency, which was defined as the time when the activity varied by ≥2SDs from the baseline activity measured in the 400 ms preceding the stimulus onset. Latencies varied from 50 to 293 ms with a mean of 66 ms. Delay activity was derived from a 900-ms interval after stimulus offset shifted by 200 ms.

Most neurons in both the IPS and PFC show a phasic response early after stimulus onset and late during the memory phase. Both the sample and the delay activity were thus analyzed in two windows of 400 ms (sample) and 450 ms (delay), respectively, to account for early and late responses. A two-way ANOVA ($P < 0.01$) was calculated separately for the numerosity and length protocol for each neuron. Factors were quantity (numerosities 1 to 4 or lines with lengths of 0.85, 1.7, 2.55, or 3.4° of visual angle, respectively) and stimulus type (standard or control).

Sharpness and strength of selectivity

We computed a selectivity-strength index (S_{st}) for each neuron by using the formula

$$S_{st} = \frac{FR_{max} - FR_{min}}{FR_{max} + FR_{min}} \quad (1)$$

where FR_{max} is the maximum firing rate of the neuron (to the preferred stimulus) and FR_{min} is the minimum firing rate of the neuron (in response to the least preferred stimulus). High values of this index (closer to 1) indicate stronger selectivity.

To assess the sharpness of the selectivity, we computed in addition a selectivity-sharpness index (S_{sh})

$$S_{sh} = FR_{max} - FR_{median} \quad (2)$$

where FR_{median} is the median value of the distribution of average firing rates of the neuron to the four quantities (numerosities and lengths, respectively) presented. This index thus takes into account the responses of the neuron to each of the four quantities, as opposed to the strength of selectivity index, which takes into account only the preferred and the least preferred of the stimuli. High values of the sharpness of selectivity index indicate sharper tuning for the preferred stimulus versus any of the other stimuli.

Time course of quantity selectivity

To assess the time course of the selectivity, a sliding-window receiver operating characteristic (ROC) analysis, derived from signal detection theory (Green and Swets 1966), was used. It was performed separately for the numerosity and length protocols, respectively. Each selective neuron was tested individually, with only the response to preferred and least preferred quantities as ROC parameters.

Distribution of the discharge rates of the neuron for each presentation of the preferred quantity (real positives) was tested against distribution of the discharge rates of the same neuron for each trial in which the least preferred quantity was presented (false positives). The area under the ROC curve (AUC) thus obtained was used as a measure of the selectivity of the neuron for that quantity type. Values of 0.5 indicate chance-level discrimination between the stimuli (no selectivity), whereas values of 1 denote perfect classification.

To assess the time course of the quantity selectivity in the neuronal activity, we computed the AUC in a 50-ms window that was slid in 1-ms steps. The AUC values obtained were compared with the null distribution obtained by shuffling all trials, regardless of the condition, at a threshold of 99%. We thus assessed the selectivity profile of the neuronal activity beginning 500 ms prior to the sample onset (in the fixation period) and ended with the end of the delay period (coinciding with the test stimulus onset, when the monkeys were allowed to freely move their eyes). We performed this for each quantity-selective neuron.

We computed the mean AUC values for each recording area (IPS and PFC), each protocol period (sample phase and delay phase), and each stimulus type (numerosity and length) by averaging the AUC values obtained within the last 700 ms of the sample phase and the last 800 ms of the delay phase, respectively, for each individual neuron. We compared the distributions of the mean AUC values obtained for neurons discriminating numerosity versus length, during the sample versus the delay phase, and recorded within the IPS versus the PFC, and tested each of these distributions with *t*-tests.

We defined the latency of the selectivity for each neuron as the time (in milliseconds) after sample stimulus onset, but no later than 300 ms after stimulus onset, for which the ROC values of 20 consecutive windows (of 50 ms, slid by 1 ms) exceeded the 99% upper threshold of the null distribution obtained through Monte Carlo simulations on all trials and all conditions for each individual neuron separately.

RESULTS

Behavioral performance

We trained two monkeys in a delayed match-to-sample (DMS) task to discriminate continuous and discrete quantities in two protocols (Tudusciuc and Nieder 2007). In the "length protocol" (Fig. 1*A*), the monkey had to discriminate the length of a line (continuous-spatial quantity), which could have one of four values. In the "numerosity protocol" (Fig. 1*B*), the number of (one to four) items in multiple-dot displays (discrete-numerical quantity) was the relevant stimulus dimension. To ensure that the monkeys solved the task based on the relevant quantitative information (length or numerosity, respectively), other covarying features of the stimuli (i.e., the total area for the line stimuli, the total area, and thus also luminance and contrast, total circumference, the density, and the geometrical configuration for the numerosity stimuli) were controlled and the positions of the dots and lines were greatly varied (Nieder et al. 2002) (see METHODS for details).

During the initial behavioral training, the monkeys discriminated up to nine different line lengths in one session, demonstrating that they treated line lengths as a continuous dimension (see Fig. 2*A* in Tudusciuc and Nieder 2007). For recording, however, we restricted the quantity dimensions to four lengths and numerosities 1 to 4, respectively, to obtain a sufficient number of trial repetitions for each stimulus condition. Both monkeys correctly solved 81–99% of the trials for both the length and the numerosity protocols ($P < 0.001$ compared with chance, binomial test), regardless of the controls used.

General firing properties

We analyzed the activity of 400 single units from the depth of the IPS and 635 single units from the lateral prefrontal

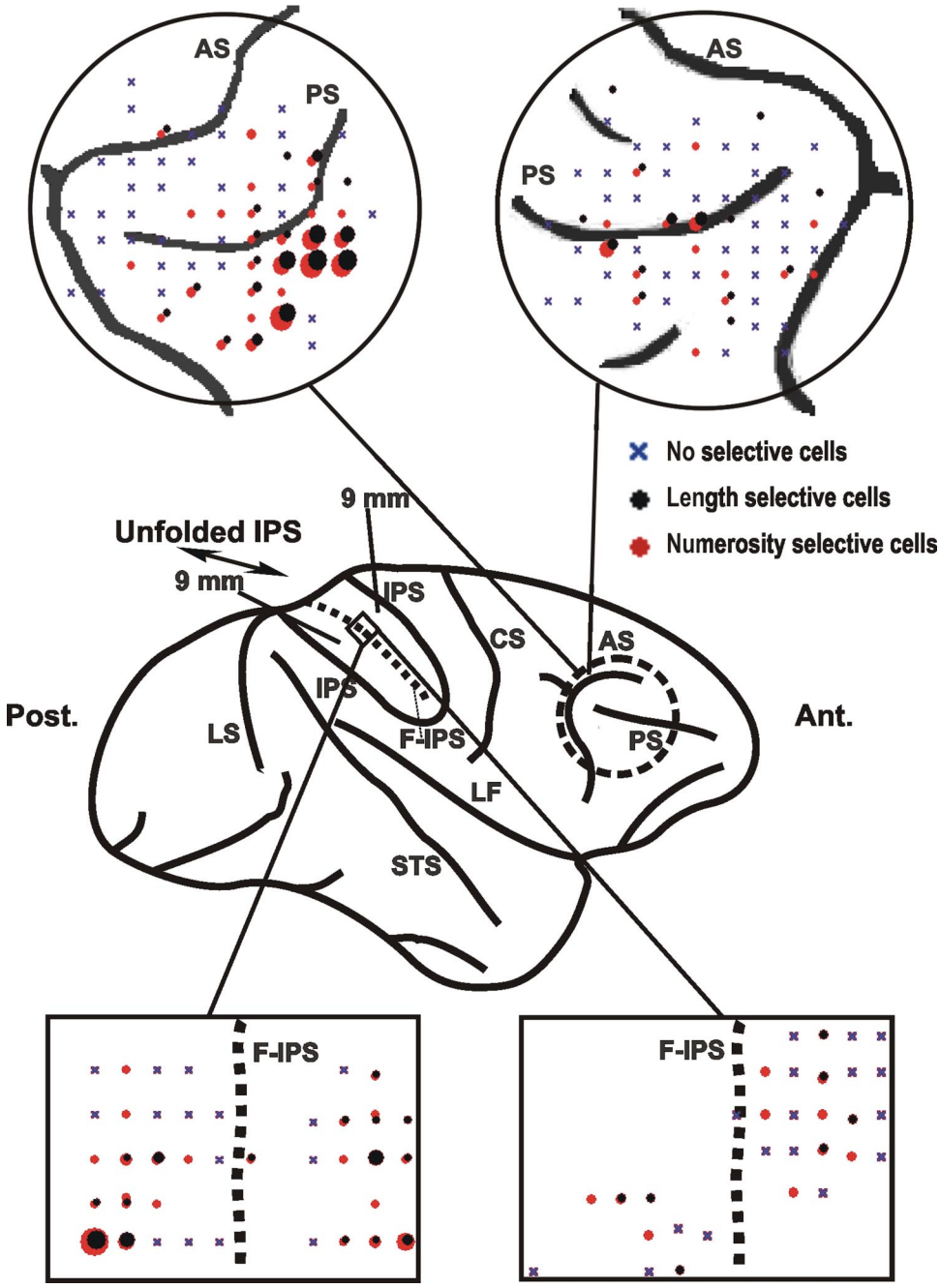

FIG. 2. Location of recording sites in the prefrontal and parietal cortices of the 2 monkeys. The *middle panel* shows a lateral view of a monkey brain, with the anterior (frontal) pole on the *right*, highlighting the relevant anatomical structures. The intraparietal sulcus is depicted unfolded. The *top circular panels* represent the prefrontal locations, in a right (monkey M) and a left (monkey H) hemisphere, respectively. The *bottom quadratic panels* represent the recording locations in the depth of the intraparietal sulcus of the monkeys, one in the right hemisphere (monkey M) and one in the left hemisphere (monkey H). The dot size reflects the number of selective neurons recorded at each location (from 1 to 7). AS, arcuate sulcus; CS, central sulcus; IPS, intraparietal sulcus; F-IPS, fundus of the IPS; LF, lateral fissure; LS, lunate sulcus; PS, principal sulcus; STS, superior temporal sulcus.

cortex (LPFC) of two monkeys while they performed the DMS task. Neurons from the depth of the IPS and from the LPFC were recorded simultaneously to ensure identical task-performance conditions. The data were collected from the right hemisphere over 48 recording sessions for monkey M and from the left hemisphere over 25 recording sessions for monkey H. Figure 2 shows a detailed anatomical map of the recording sites, for each monkey and each area.

We tested the neurons' selectivity to the quantity stimuli with a two-factor ANOVA, which we applied separately for the sample and for the delay periods. To account for the phasic and/or sustained responses that many neurons showed after stimulus onset, we performed the analysis in two windows for each period (see METHODS). Neurons showing main effects of length (or numerosity, respectively), with no effect of protocol type (standard or control) or factor interaction, were defined as quantity-selective neurons (two-way ANOVA, $P < 0.01$). Many of the recorded neurons selectively increased their firing rates in response to the quantity stimuli we presented. Figure 3 shows two example neurons that were selective for quantity in the sample period (Fig. 3, *A* and *B*) and two others that were selective during the delay period (Fig. 3, *C* and *D*). A small proportion of these neurons encoded one continuous and one discrete quantity.

Quantity selectivity (i.e., both length and numerosity selectivity together) was similar in both cortical areas. In the IPS, 104 of 400 neurons were quantity selective and 194 of 635 neurons in the PFC (26% in the IPS vs. 31% in the PFC, χ^2 test, $P > 0.05$). Comparable proportions of these neurons in the respective areas were selective during the sample period, when the monkey was presented with the relevant quantity stimulus, and during the delay

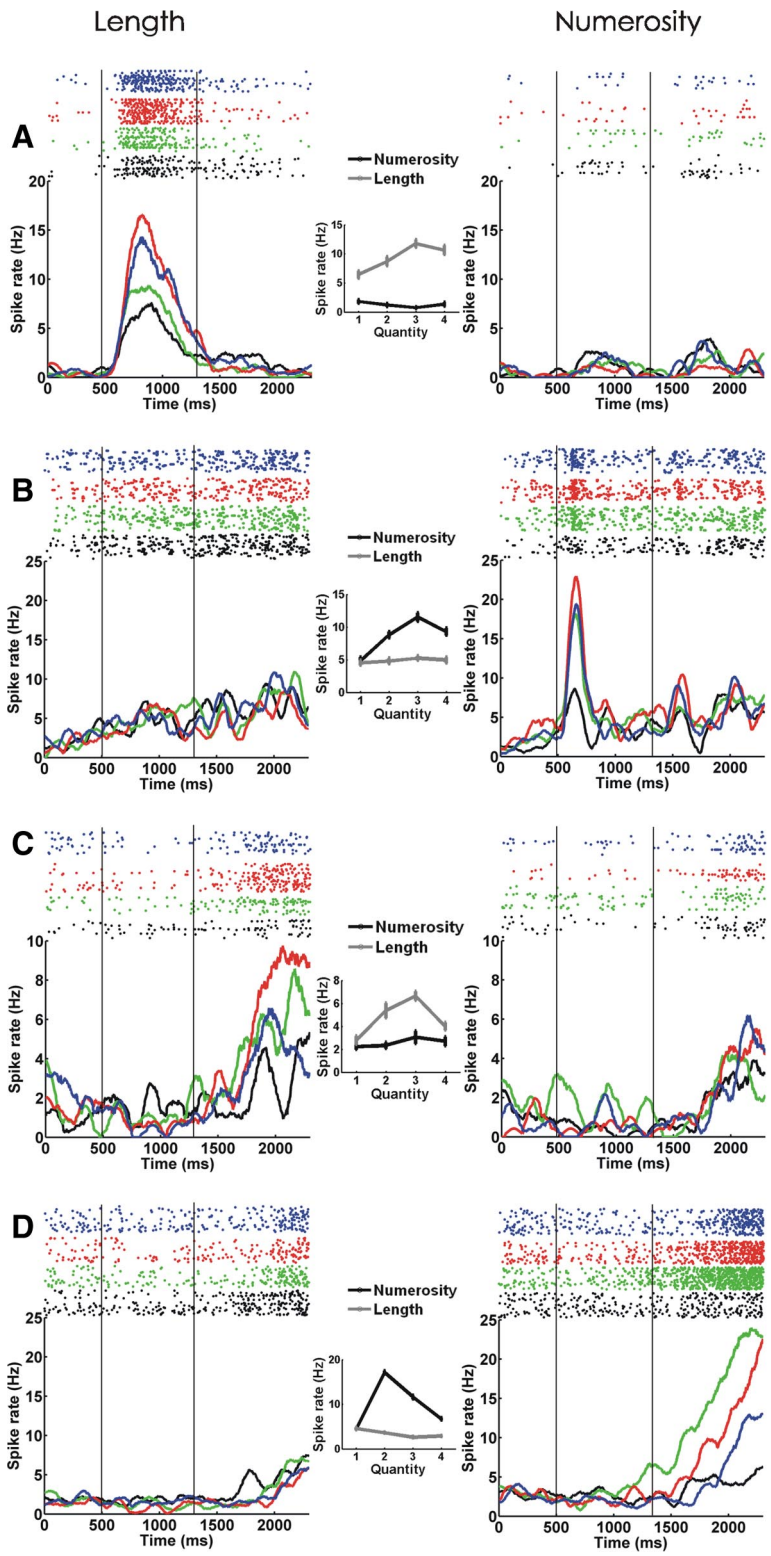

FIG. 3. Example neurons exhibiting selectivity for quantity. *A*: parietal neuron tuned to the second longest line length, but not to numerosity in the sample phase. *Left* and *right panels* illustrate the discharge rates of the same neuron in the length and numerosity protocol, respectively. In the *top panels,* the neuronal responses are plotted as dot-raster histograms (each dot represents an action potential in response to the quantity, as illustrated by example stimuli to the *left* and is color-coded accordingly); corresponding averaged spike density functions are shown in the *bottom panels* (activity to a given quantity averaged over all trials and smoothed by a Gaussian kernel of width 150 ms). The first 500 ms represent the fixation period. The area between the 2 black vertical bars represents the sample stimulus presentation period; the following 1,000 ms indicate the delay phase. Colors correspond to the quantity dimensions. *Inset*: tuning functions for the firing rates of the neuron in response to line length and numerosity stimuli during the sample phase. *B*: parietal neuron tuned to numerosity 3 in the sample period, but not to any tested length. *C*: prefrontal neuron tuned to the 3rd length in the delay period. *D*: prefrontal neuron tuned to numerosity 2 in the delay phase. For *B*, *C*, and *D* the layout is the same as in *A*. The *insets* in *C* and *D* represent the tuning functions over the delay period.

period in which the monkeys had to keep quantity information in memory for subsequent comparison with the test stimulus [72 (69%) sample-selective neurons vs. 59 (57%) delay-selective neurons in IPS and for the PFC 120 (62%) sample-selective neurons vs. 131 (68%) delay-selective ones, χ^2 test, $P > 0.05$].

In the prefrontal populations, 109 of the 635 recorded cells (17% of the total sample) selectively increased their firing rates in response to line length. Of those, 67 neurons were selectively tuned to length during the sample period and 68 neurons during the delay period. The distribution of selective neurons over the two types of quantity stimuli for the prefrontal and the parietal populations is depicted in Fig. 4. The proportion of IPS neurons encoding both lengths and numerosity during the sample phase (Fig. 4*A*) was similar to that in the PFC (Fig. 4*C*)

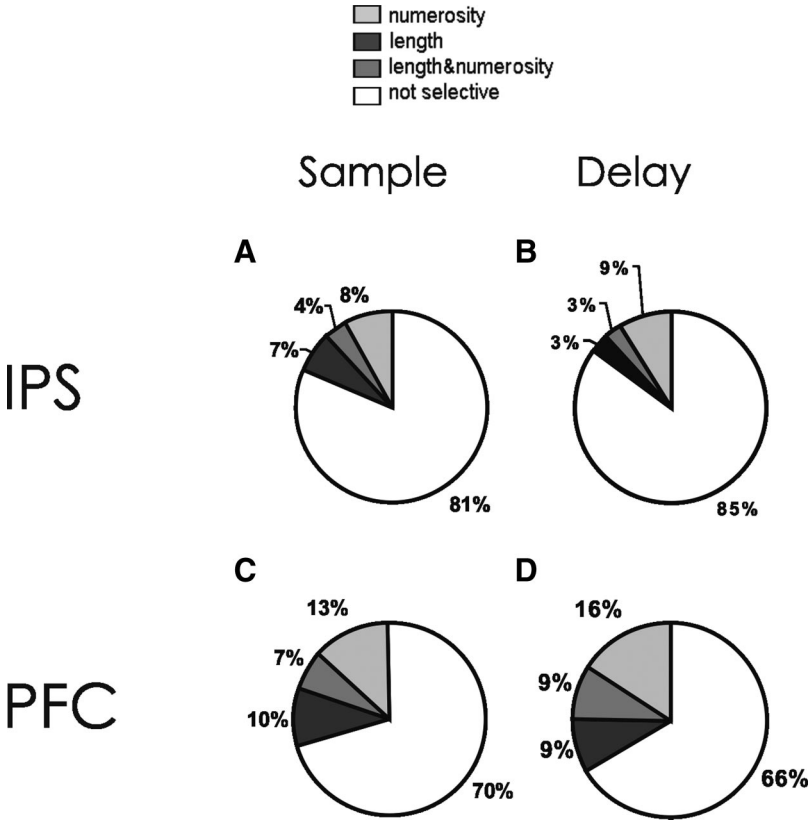

FIG. 4. Distribution of the quantity-selective neurons. The pie diagrams show the percentages of selective neurons distributed over recording area (IPS on the 2 *top plots* vs. prefrontal cortex [PFC] on the 2 *bottom plots*), trial period (sample on the *left* vs. delay on the *right*), and protocol (length vs. numerosity discrimination).

(19% in the IPS vs. 26% in the PFC, χ^2 test, $P > 0.05$). The same was true for the delay period [20% for the IPS (Fig. 4*B*) vs. 21% for the PFC (Fig. 4*D*), χ^2 test, $P > 0.05$]. Furthermore, similar proportions of neurons were tuned to each of the four presented quantities for each protocol, in sample and delay, for the IPS and the PFC populations (Fig. 5).

To further investigate whether the IPS population exhibited a higher number of neurons that encode quantity in the sample period than that in the PFC, we compared the number of selective neurons in each of the two windows defined for the ANOVA analysis described earlier. The results, presented in Table 1, show that there were indeed significantly more neurons tuned to quantity in the IPS during the early sample phase than in the PFC (76% IPS vs. 54% PFC, χ^2 test, $P < 0.01$), especially to the length stimuli (see Table 2).

The tuning functions for both length and numerosity peaked at the preferred quantity and showed a decrease in activity with increasing distance from it. Thus our data support a labeled-

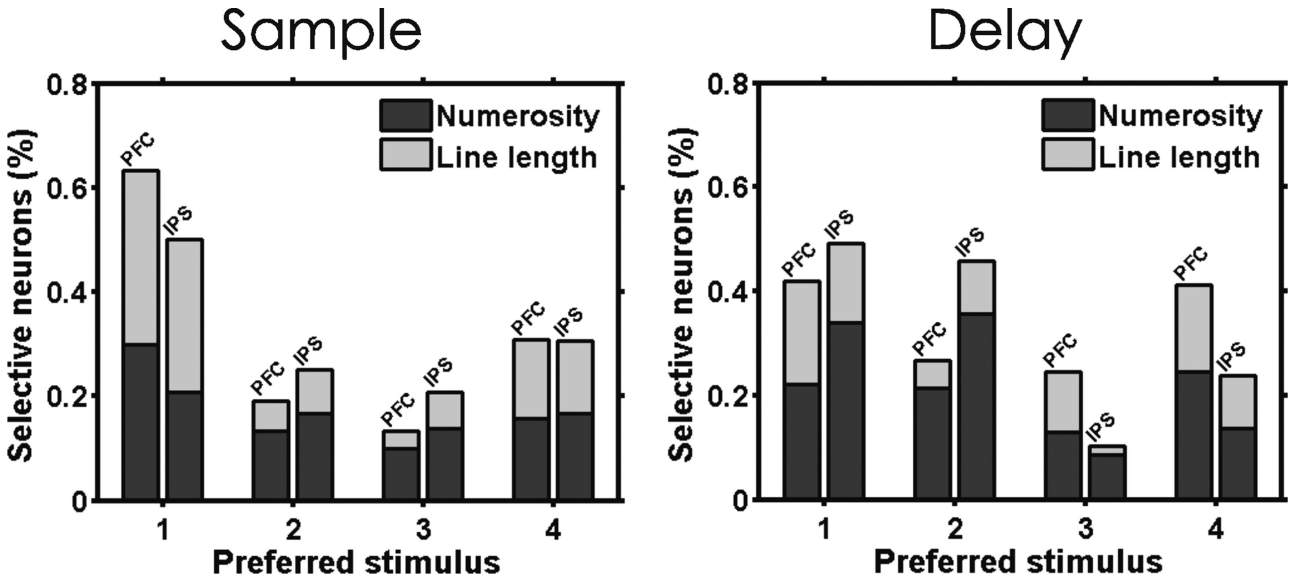

FIG. 5. Proportions of neurons selective for each stimulus. The bar diagrams indicate the proportion of cells selective for each of the stimulus types. The *left panel* shows the respective proportions of sample-selective neurons, the *right panel* delay-selective neurons. The preferred quantities are on the *x*-axis. The quantity types are color-coded (dark gray for numerosities and light gray for lengths). IPS, intraparietal sulcus; PFC, prefrontal cortex.

TABLE 1. *Distribution of the early versus late selective neurons in the IPS and PFC*

	Analysis Window	IPS	PFC	χ^2
Sample	Early period (400 ms)	55 (76%)	65 (54%)	$P < 0.01$
	Late period (400 ms)	39 (54%)	79 (66%)	n.s.
Delay	Early period (450 ms)	28 (47%)	67 (51%)	n.s.
	Late period (450 ms)	43 (73%)	99 (76%)	n.s

n.s.: nonsignificant, $P > 0.05$.

line code for continuous quantities in the PFC, as well (Fig. 6, *A* and *B*). Previous studies already evidenced that this type of quantity codes is present in the IPS for continuous and discrete quantities (Tudusciuc and Nieder 2007) and in the PFC for discrete quantities (Nieder and Miller 2004). The shapes of the tuning functions obtained for neurons coding for continuous quantities were comparable to those obtained for numerosity encoding neurons (Fig. 6, *C–F*), for sample as well as delay in the PFC as well.

Strength and sharpness of selectivity to quantities

We further investigated the quantity selectivity properties in the two neuronal populations by computing for each neuron individually a selectivity-strength index (S_{st}), measuring the strength of selectivity (see METHODS). This was done separately for the numerosity and the length stimuli. The results are depicted in Fig. 7, *A* (for the IPS) and *C* (for the PFC). There was no significant difference between the index values for lengths versus numerosities in either area (IPS and PFC) and either period (sample and delay): IPS sample length $S_{st} = 0.37$, numerosity $S_{st} = 0.39$, Mann–Whitney *U* test, $P > 0.05$; IPS delay length $S_{st} = 0.16$, numerosity $S_{st} = 0.18$, $P > 0.05$; PFC sample length $S_{st} = 0.53$, numerosity $S_{st} = 0.52$, $P > 0.05$; PFC delay length $S_{st} = 0.37$, numerosity $S_{st} = 0.41$, $P > 0.05$. Therefore we pooled the index values for the two quantities and obtained distributions of index values for quantity in two areas (IPS and PFC) and two trial periods (sample and delay). For both the IPS (Fig. 7*A*) and the PFC (Fig. 7*C*), the index values in the sample period exceeded those in the delay period (IPS sample $S_{st} = 0.38$, IPS delay $S_{st} = 0.17$, Mann–Whitney *U* test, $P < 0.05$; PFC sample $S_{st} = 0.53$, PFC delay $S_{st} = 0.39$, Mann–Whitney *U* test, $P < 0.05$). Furthermore, the index values in the PFC exceeded those in the IPS, both during the sample (IPS $S_{st} = 0.38$, PFC $S_{st} = 0.53$, Mann–Whitney *U* test, $P < 0.05$) and during the delay period (IPS $S_{st} = 0.17$, PFC $S_{st} = 0.39$, Mann–Whitney *U* test, $P < 0.05$), indicating that PFC neurons encode quantities with more sensitivity and strength than the IPS population.

The strength of selectivity index uses only two of the four stimuli presented in each protocol: the preferred and the least preferred ones. Although this measure gives an accurate account of the power of the tested neuron to discriminate its preferred stimulus from the least preferred one (thus the strength of its selectivity for the preferred quantity), it fails to give a measure of how well the neuron can discriminate its preferred quantity from a group of other stimuli closely resembling the preferred stimulus. Therefore we computed a selectivity-sharpness index (S_{sh}) for quantifying the width of the selectivity curve (see METHODS), taking into account the median firing rate of the neuron to all the four quantity stimuli presented. The average S_{sh} is shown in Fig. 7, *B* and *D* (for the IPS and PFC populations of selective neurons, respectively). We first compared the average index values for length versus numerosity selectivity and found no differences between them in either period or area: IPS sample length $S_{sh} = 4.73$, numerosity $S_{sh} = 3.67$, Mann–Whitney *U* test, $P > 0.05$; IPS delay length $S_{sh} = 1.45$, numerosity $S_{sh} = 1.47$, $P > 0.05$; PFC sample length $S_{sh} = 2.02$, numerosity $S_{sh} = 2.29$, $P > 0.05$; PFC delay length $S_{sh} = 1.35$, numerosity $S_{sh} = 1.81$, $P > 0.05$. Therefore we pooled the data (continuous and discrete quantities taken together) and compared the average index values across areas and trial periods.

The average selectivity-sharpness index (S_{sh}) values were higher for the sample period than those for the delay period, both in the IPS population (sample $S_{sh} = 4.20$, delay $S_{sh} = 1.46$, Mann–Whitney *U* test, $P < 0.01$) and in the PFC population (sample $S_{sh} = 2.16$, delay $S_{sh} = 1.58$, Mann–Whitney *U* test, $P < 0.05$)—i.e., the neurons are more sharply tuned to their preferred quantity during the sample phase and thus better discriminating their preferred quantity from other close quantities than during the delay phase.

For the IPS neurons, average S_{sh} in the sample phase was significantly higher than that for PFC neurons (IPS $S_{sh} = 4.20$, PFC $S_{sh} = 2.16$, Mann–Whitney *U* test, $P < 0.01$). This indicates that IPS neurons can better discriminate their preferred quantity from the presented set of quantities than the PFC neurons. During the delay period, however, there was no difference between the two areas (IPS $S_{sh} = 1.46$, PFC $S_{sh} = 1.58$, Mann–Whitney *U* test, $P > 0.05$).

Time course of quantity discriminability

To further assess the differences in the firing properties of prefrontal versus parietal neurons engaged in the discrimination of quantities, we analyzed the temporal dynamics of the neurons' quantity discriminability by means of a sliding-window receiver operating characteristic (ROC) analysis and derived the area under the ROC curve (AUC). We included all quantity-selective neurons (ANOVA, $P < 0.01$; see METHODS). The results, as displayed in Fig. 8, show the time course of the average selectivity for quantity over the IPS and PFC populations, for the numerosity and for the length stimuli separately. Sample-selective (Fig. 8, *A* and *C*) and delay-selective neurons (Fig. 8, *B* and *D*) were grouped together. (Note that some neurons were selective during both the sample and the delay period as well.)

The discriminability (i.e., AUC values) within a given area (IPS or PFC) or test phase (sample or delay) was similar for

TABLE 2. *Distribution of sample- versus delay-selective neurons and of neurons selective during both the sample and delay phase of each protocol in the IPS and PFC*

	Stimulus Type	IPS	PFC	χ^2
Length	Sample only	31 (58%)	41 (38%)	$P < 0.05$
	Delay only	13 (25%)	42 (39%)	n.s
	Both sample and delay	9 (17%)	26 (24%)	n.s
Numerosity	Sample only	31 (39%)	39 (29%)	n.s.
	Delay only	34 (42%)	57 (42%)	n.s
	Both sample and delay	15 (19%)	40 (29%)	n.s

n.s.: nonsignificant, $P > 0.05$.

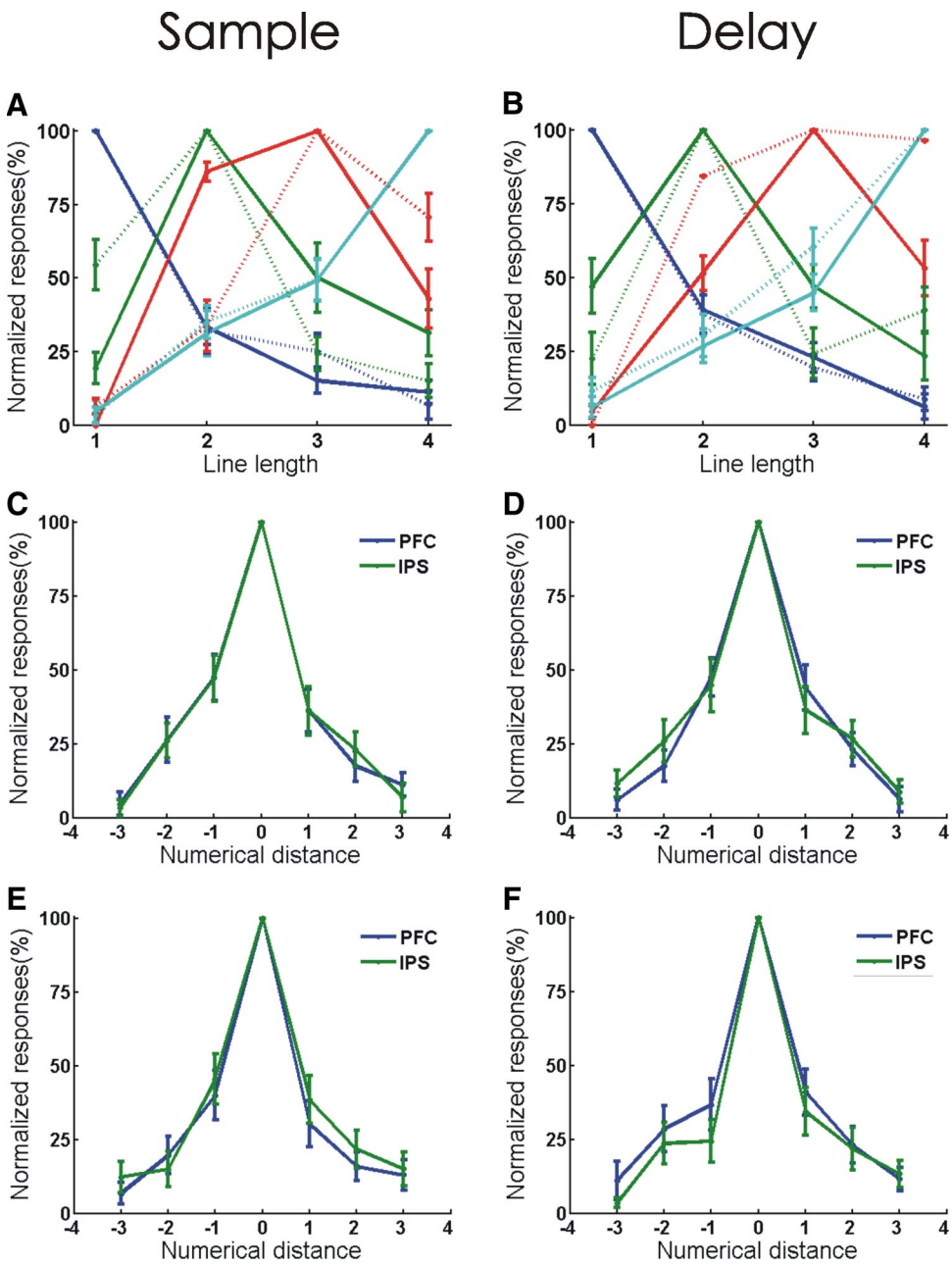

FIG. 6. Selectivity tuning functions. *A* and *B*: the normalized responses averaged for neurons with the same preferred length are plotted separately for neurons recorded in the IPS (dotted lines) and PFC (solid lines). Just as the IPS neurons, all PFC neurons showed a progressive drop-off of the response with increasing distances from the preferred length. *C–F*: normalized activity of the PFC and IPS neurons for the continuous quantities (*C* and *D*) and discrete quantities (*E* and *F*) as a function of distance from the preferred quantity, for both sample (*C* and *E*) and delay (*D* and *F*).

line and numerosity representations, respectively (*t*-test, $P > 0.05$); only in the delay phase, numerosity-selective neurons tended to show a higher AUC ($P = 0.05$). Between areas, discriminability in the sample phase was considerably higher (0.57 mean AUC for length in the IPS vs. 0.51 in the PFC and 0.59 mean AUC for numerosity in the IPS vs. 0.52 in the PFC) for IPS neurons compared with PFC neurons (*t*-test, $P < 0.05$); interestingly, such a difference was not present in the delay period ($P > 0.05$).

To determine more temporal response characteristics, we computed the latency of the selectivity onset, as measured with the ROC sliding-window analysis, for each selective neuron. For statistical reasons, we determined the ROC values in windows of 50 ms and also performed Monte Carlo simulations with these parameters for all conditions to construct a null distribution for every neuron. (Neurons showing selectivity to both the length and the numerosity stimuli were excluded.) There was a significant difference in latency between the length-selective and the numerosity-selective neurons, both in the IPS (length median latency 315 ms; numerosity median latency 198.5 ms, Mann–Whitney *U* test, $P < 0.05$) and in the PFC population (length median latency 122 ms; numerosity median latency 248 ms, Mann–Whitney *U* test, $P < 0.05$). When comparing the IPS population (length-selective and numerosity-selective neurons together) to the PFC population of sample-selective neurons, we found that the IPS neurons reached the selectivity criterion faster than did the PFC neurons (the latency of only 41 IPS and 51 PFC sample-selective neurons could be determined). The IPS median latency was 199.5 ms, whereas the PFC median latency reached 211 ms (Mann–Whitney *U* test, $P > 0.01$) (Fig. 9).

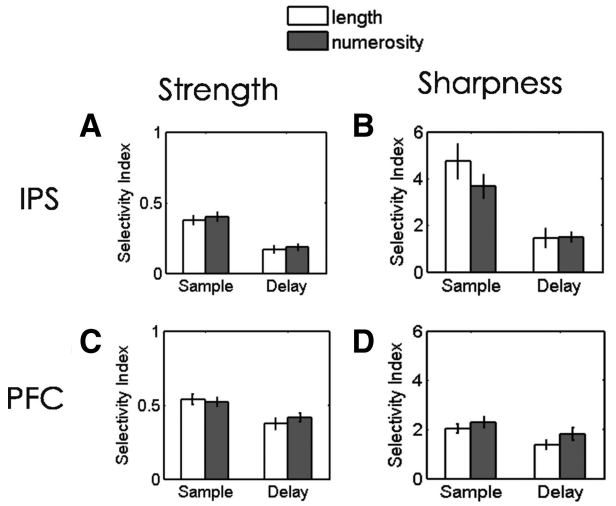

FIG. 7. Selectivity indices. *A* and *B*: average index values for the strength of selectivity for the parietal (*A*) and prefrontal (*B*) areas. The white bars correspond to length stimuli, the gray bars to numerosity stimuli. Error bars represent the SE for each distribution. *C* and *D*: average index values for the sharpness of selectivity for the parietal (*C*) and prefrontal (*D*) populations. Layout is the same as that in *A* and *B*.

DISCUSSION

We have simultaneously recorded single-unit activity in the prefrontal and parietal cortices of two monkeys while they were engaged in continuous (length) and discrete (numerosity) quantity discrimination. This enabled us to systematically analyze the similarities and differences in the coding dynamics of quantity-selective neurons in these two brain areas. The parietal and prefrontal neurons shared many properties in their activity in response to continuous and discrete quantity stimuli. However, subtle differences between these two areas hint toward specialized roles for each brain area in magnitude discrimination.

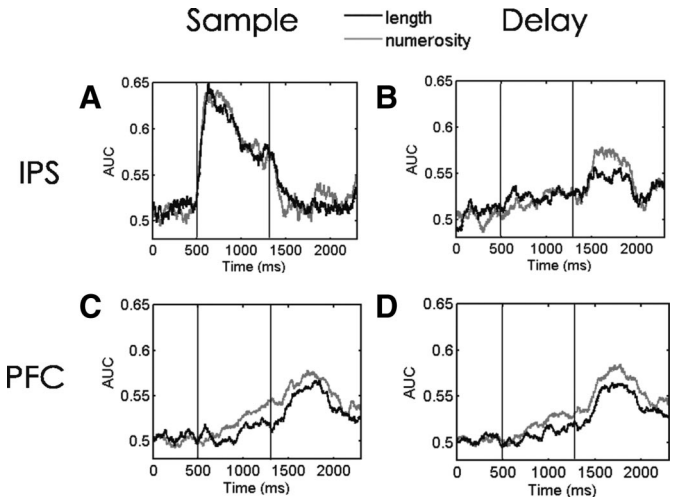

FIG. 8. Average area under the receiver operating characteristic (ROC) curve (AUC) for the sliding-window ROC analysis. The mean AUC values for the length (in black) and numerosity (in gray) protocols computed in a sliding window (100 ms, step size 1 ms) from the beginning of the fixation period (*time 0* on the *x*-axis) to the end of the delay period (the sample period starts at 500 ms and ends at 1,300 ms and is marked by the 2 vertical bars). The average over the sample-selective neurons (*A* and *C*) is plotted separately from the average over the delay-selective ones (*B* and *D*). The parietal population data are depicted in *A* and *B*, whereas the prefrontal data are in *C* and *D*.

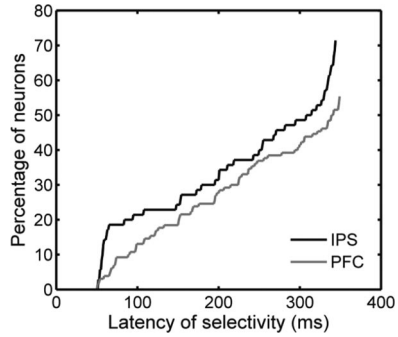

FIG. 9. Comparison of the latency of discriminability for parietal and prefrontal neurons. The diagram depicts the cumulative distributions of latencies of the onset of quantity discriminability following onset of sample stimulus for all selective neurons for which latency could be determined according. Each curve represents the percentage of neurons (on the *y*-axis) with significant quantity discriminability at the given time (on the *x*-axis) after sample stimulus onset. The latency was defined as the time (in milliseconds) after sample stimulus onset, but no later than 350 ms after stimulus onset, for which the ROC values of 50 consecutive windows (of 50 ms, slid by 1 ms) exceeded the upper 99th percentile of the null distribution, as determined by Monte Carlo simulations (see METHODS). For some neurons, the latency could not be determined.

Continuous versus discrete quantity representations within IPS and PFC

The representation of length and numerosity was surprisingly similar within the IPS and PFC, even though different sets of neurons coded these quantities. First, the respective proportions of neurons coding length and numerosity were comparable in the IPS and the PFC. Second, both the selectivity-strength index (S_{st}) and the selectivity-sharpness index (S_{sh}) reached similar values for length and numerosity tuning curves. Third, there was no difference in discriminability (as measured by AUC values) of IPS and PFC neurons for line and numerosity representations.

Neurons coding either length or numerosity, or both, were anatomically intermingled in the PFC and the IPS. These results indicate that neurons coding spatial and numerical quantities are not grouped within a unique, well-defined anatomical location. Rather, such neurons are relatively distributed and within the PFC and along the IPS fundus. These data from macaques are in agreement with a recent functional imaging study proposing a distributed overlapping code for continuous quantity dimension in humans (Pinel et al. 2004). They support the idea of the PFC and the IPS as two important poles of a broader network of areas involved in nonnumerical magnitude representation (Castelli et al. 2006; Fias et al. 2003; Kaufmann et al. 2005) and in temporal information representation (Onoe et al. 2001).

Quantity coding between IPS and PFC

The neurons' quantity (length and numerosity together) coding properties across IPS and PFC showed many commonalities. For both the IPS and the PFC, the selectivity-strength index (S_{st}) values in the sample period exceeded those in the delay period. Similarly, the average selectivity-sharpness index (S_{sh}) values were higher for the sample period than for the delay period, both in the IPS population and in the PFC population.

However, pronounced differences between the IPS and PFC were also present. Early during the sample period, a higher

ratio of IPS neurons represented quantity. In addition, the average selectivity-sharpness index (S_{sh}) of IPS neurons in the sample phase was significantly higher than that for PFC neurons. The most pronounced difference was related to the discriminability between the best and least preferred quantities, as determined by the AUC values from the ROC analysis. Discriminability in the sample phase was much higher for IPS neurons, both for length and numerosity. In addition, IPS neurons dissociated the best and least preferred stimuli almost 40 ms earlier than PFC neurons. In other words, IPS neurons became quantity selective much earlier than did PFC neurons.

The finding that IPS neurons respond earlier to quantity is in agreement with a previous analysis of numerosity selectivity (Nieder and Miller 2004). Both studies strongly indicated that the visual quantity might be first extracted in the IPS, then conveyed to the PFC. Together with the higher discriminability in the IPS during the sample period, it reflects a more active role of parietal neurons in extracting the quantity information from the visually presented stimulus. In the PFC, this activity might be expanded, enhanced, and held on-line in working memory for further decisional processes. The very similar response characteristics of IPS and PFC neurons during magnitude processing reflect anatomical and functional connections (Schwartz and Goldman-Rakic 1984). Temporary inactivation of one region changes the response properties of neurons in the other (Chafee and Goldman-Rakic 2000; Quintana et al. 1989), suggesting close functional interdependence between the two regions. This interdependence is not only seen during the encoding of the stimuli, but also by the comparable degree of delay activity in both areas. This indicates both the IPS and PFC as important nodes for the encoding and working memory of quantitative information (Fuster 1973, 1997; Goldman-Rakic 1995). However, with the exception of the first appearance of quantity-related activity, the subsequent flow of information between these association cortices remains elusive. Recurrent connections between the IPS and the PFC (Barash 2003) prevent a precise determination of the respective contributions of each area by analyzing single-unit activity alone, although interesting insights could be obtained by recording the local field potentials as well, and by following the flow of information between the two areas.

Coding scheme for continuous and discrete quantities in the prefrontal cortex

In both the IPS and PFC, with respect to the line-length stimuli, our monkeys had to discriminate elicited peak-tuned tuning function to the preferred length—i.e., they showed a gradual decrease in firing rate with increasing distance to the preferred stimulus. The representational scheme for spatial quantity thus is a *labeled-line code*, consisting in populations of neurons tuned to specific magnitude values. A labeled-line code was also previously described for neurons representing numerosity in the IPS and PFC (Nieder and Merten 2007; Nieder and Miller 2003, 2004; Nieder et al. 2002).

This result contrasts the "monotonic stimulus encoding" idea proposed by Romo and colleagues (Brody et al. 2003; Romo et al. 1999), who found neurons in the PFC that discharged as an increasing or decreasing monotonic function of the magnitude of a vibrotactile stimulus; similar results were also obtained with visual stimuli, in a task that required the choice of the brighter of two stimuli varying in luminance (Constantinidis et al. 2001). Moreover, Roitman et al. (2007) observed monotonic coding in most lateral intraparietal cortex neurons in monkeys implicitly representing numerosity (i.e., numerosity was informative for the monkeys, but they did not have to discriminate it). Our data recorded in monkeys explicitly judging set size, however, support a labeled-line code for both spatial and numerical quantities. The reasons for these discrepancies remain a subject for further investigations.

Interestingly, a labeled-line code for numerosity has also been suggested in the human cortex by a previous imaging study applying a functional magnetic resonance imaging adaptation protocol (Piazza et al. 2004). Here, the tuning characteristics of a population of neurons can indirectly be read out by blood oxygenation level–dependent (BOLD) signal adaptation and recovery effects. The subjects were repeatedly presented with a set of dots displaying the same numerosity (e.g., 16 dots). This caused a gradual decrease in the BOLD signal, supposedly caused by numerosity-selective neurons getting "habituated." When deviant numerosities (e.g., 8 dots) were subsequently shown, a recovery from BOLD signal adaptation was observed. The authors then analyzed the level of recovery as a function of numerical distance between the habituation stimulus and the deviant stimulus and found that this function described an inverted Gaussian similar to the tuning functions of quantity-selective neurons we found for our stimuli. Based on our finding that spatial extent is also encoded by peak-tune tuning functions, we would predict that a very similar adaptation effect and subsequent read-out of the BOLD signal could be found for continuous quantities in the human cortex.

REFERENCES

Astafiev SV, Shulman GL, Stanley CM, Snyder AZ, Van Essen DC, Corbetta M. Functional organization of human intraparietal and frontal cortex for attending, looking, and pointing. *J Neurosci* 23: 4689–4699, 2003.

Barash S. Paradoxical activities: insight into the relationship of parietal and prefrontal cortices. *Trends Neurosci* 26: 582–589, 2003.

Bisley JW, Goldberg ME. Neuronal activity in the lateral intraparietal area and spatial attention. *Science* 299: 81–86, 2003.

Brody CD, Hernandez A, Zainos A, Romo R. Timing and neural encoding of somatosensory parametric working memory in macaque prefrontal cortex. *Cereb Cortex* 13: 1196–1207, 2003.

Buhusi CV, Meck WH. What makes us tick? Functional and neural mechanisms of interval timing. *Nat Rev Neurosci* 6: 755–765, 2005.

Castelli F, Glaser DE, Butterworth B. Discrete and analogue quantity processing in the parietal lobe: a functional MRI study. *Proc Natl Acad Sci USA* 103: 4693–4698, 2006.

Chafee MV, Goldman-Rakic PS. Inactivation of parietal and prefrontal cortex reveals interdependence of neural activity during memory-guided saccades. *J Neurophysiol* 83: 1550–1566, 2000.

Cohen Kadosh R, Cohen Kadosh K, Schuhmann T, Kaas A, Goebel R, Henik A, Sack AT. Virtual dyscalculia induced by parietal-lobe TMS impairs automatic magnitude processing. *Curr Biol* 17: 689–693, 2007.

Colby CL, Goldberg ME. Space and attention in parietal cortex. *Annu Rev Neurosci* 22: 319–349, 1999.

Constantinidis C, Franowicz MN, Goldman-Rakic PS. The sensory nature of mnemonic representation in the primate prefrontal cortex. *Nat Neurosci* 4: 311–316, 2001.

Dehaene S, Molko N, Cohen L, Wilson AJ. Arithmetic and the brain. *Curr Opin Neurobiol* 14: 218–224, 2004.

Dehaene S, Sergent C, Changeux JP. A neuronal network model linking subjective reports and objective physiological data during conscious perception. *Proc Natl Acad Sci USA* 100: 8520–8525, 2003.

Dehaene S, Spelke E, Pinel P, Stanescu R, Tsivkin S. Sources of mathematical thinking: behavioral and brain-imaging evidence. *Science* 284: 970–974, 1999.

Eger E, Sterzer P, Russ MO, Giraud AL, Kleinschmidt A. A supramodal number representation in human intraparietal cortex. *Neuron* 37: 719–725, 2003.

Fias W, Lammertyn J, Reynvoet B, Dupont P, Orban GA. Parietal representation of symbolic and nonsymbolic magnitude. *J Cogn Neurosci* 15: 47–56, 2003.

Fuster JM. Unit activity in prefrontal cortex during delayed-response performance: neuronal correlates of transient memory. *J Neurophysiol* 36: 61–78, 1973.

Fuster JM. Network memory. *Trends Neurosci* 20: 451–459, 1997.

Genovesio A, Tsujimoto S, Wise SP. Neuronal activity related to elapsed time in prefrontal cortex. *J Neurophysiol* 95: 3281–3285, 2006.

Gobel S, Walsh V, Rushworth MF. The mental number line and the human angular gyrus. *Neuroimage* 14: 1278–1289, 2001.

Goldman-Rakic PS. Cellular basis of working memory. *Neuron* 14: 477–485, 1995.

Green DM, Swets JA. *Signal Detection Theory and Psychophysics*. Wiley: New York, 1966.

Henik A, Tzelgov J. Is three greater than five: the relation between physical and semantic size in comparison tasks. *Mem Cognit* 10: 389–395, 1982.

Hubbard EM, Piazza M, Pinel P, Dehaene S. Interactions between number and space in parietal cortex. *Nat Rev Neurosci* 6: 435–448, 2005.

Kaufmann L, Koppelstaetter F, Delazer M, Siedentopf C, Rhomberg P, Golaszewski S, Felber S, Ischebeck A. Neural correlates of distance and congruity effects in a numerical Stroop task: an event-related fMRI study. *Neuroimage* 25: 888–898, 2005.

Leon MI, Shadlen MN. Representation of time by neurons in the posterior parietal cortex of the macaque. *Neuron* 38: 317–327, 2003.

Macar F, Anton JL, Bonnet M, Vidal F. Timing functions of the supplementary motor area: an event-related fMRI study. *Brain Res Cogn Brain Res* 21: 206–215, 2004.

Macar F, Lejeune H, Bonnet M, Ferrara A, Pouthas V, Vidal F, Maquet P. Activation of the supplementary motor area and of attentional networks during temporal processing. *Exp Brain Res* 142: 475–485, 2002.

Macar F, Vidal F. Time processing reflected by EEG surface Laplacians. *Exp Brain Res* 145: 403–406, 2002.

Medendorp WP, Tweed DB, Crawford JD. Motion parallax is computed in the updating of human spatial memory. *J Neurosci* 23: 8135–8142, 2003.

Merriam EP, Genovese CR, Colby CL. Spatial updating in human parietal cortex. *Neuron* 39: 361–373, 2003.

Nieder A. Counting on neurons: the neurobiology of numerical competence. *Nat Rev Neurosci* 6: 177–190, 2005.

Nieder A, Diester I, Tudusciuc O. Temporal and spatial enumeration processes in the primate parietal cortex. *Science* 313: 1431–1435, 2006.

Nieder A, Freedman DJ, Miller EK. Representation of the quantity of visual items in the primate prefrontal cortex. *Science* 297: 1708–1711, 2002.

Nieder A, Merten K. A labeled-line code for small and large numerosities in the monkey prefrontal cortex. *J Neurosci* 27: 5986–5993, 2007.

Nieder A, Miller EK. Coding of cognitive magnitude: compressed scaling of numerical information in the primate prefrontal cortex. *Neuron* 37: 149–157, 2003.

Nieder A, Miller EK. A parieto-frontal network for visual numerical information in the monkey. *Proc Natl Acad Sci USA* 101: 7457–7462, 2004.

Onoe H, Komori M, Onoe K, Takechi H, Tsukada H, Watanabe Y. Cortical networks recruited for time perception: a monkey positron emission tomography (PET) study. *Neuroimage* 13: 37–45, 2001.

Orban GA, Van Essen D, Vanduffel W. Comparative mapping of higher visual areas in monkeys and humans. *Trends Cogn Sci* 8: 315–324, 2004.

Piazza M, Izard V, Pinel P, Le Bihan D, Dehaene S. Tuning curves for approximate numerosity in the human intraparietal sulcus. *Neuron* 44: 547–555, 2004.

Piazza M, Pinel P, Le Bihan D, Dehaene S. A magnitude code common to numerosities and number symbols in human intraparietal cortex. *Neuron* 53: 293–305, 2007.

Pinel P, Piazza M, Le Bihan D, Dehaene S. Distributed and overlapping cerebral representations of number, size, and luminance during comparative judgments. *Neuron* 41: 983–993, 2004.

Quintana J, Fuster JM, Yajeya J. Effects of cooling parietal cortex on prefrontal units in delay tasks. *Brain Res* 503: 100–110, 1989.

Rainer G, Asaad WF, Miller EK. Selective representation of relevant information by neurons in the primate prefrontal cortex. *Nature* 393: 577–579, 1998.

Rao SM, Bandettini PA, Binder JR, Bobholz JA, Hammeke TA, Stein EA, Hyde JS. Relationship between finger movement rate and functional magnetic resonance signal change in human primary motor cortex. *J Cereb Blood Flow Metab* 16: 1250–1254, 1996.

Romo R, Brody CD, Hernandez A, Lemus L. Neuronal correlates of parametric working memory in the prefrontal cortex. *Nature* 399: 470–473, 1999.

Rossetti Y, Rode G, Pisella L, Farne A, Li L, Boisson D, Perenin MT. Prism adaptation to a rightward optical deviation rehabilitates left hemispatial neglect. *Nature* 395: 166–169, 1998.

Schwartz ML, Goldman-Rakic PS. Callosal and intrahemispheric connectivity of the prefrontal association cortex in rhesus monkey: relation between intraparietal and principal sulcal cortex. *J Comp Neurol* 226: 403–420, 1984.

Simon O, Mangin JF, Cohen L, Le Bihan D, Dehaene S. Topographical layout of hand, eye, calculation, and language-related areas in the human parietal lobe. *Neuron* 33: 475–487, 2002.

Tudusciuc O, Nieder A. Neuronal population coding of continuous and discrete quantity in the primate posterior parietal cortex. *Proc Natl Acad Sci USA* 104: 14513–14518, 2007.

Walsh V. A theory of magnitude: common cortical metrics of time, space and quantity. *Trends Cogn Sci* 7: 483–488, 2003.

Wilson FA, Scalaidhe SP, Goldman-Rakic PS. Dissociation of object and spatial processing domains in primate prefrontal cortex. *Science* 260: 1955–1958, 1993.

Zorzi M, Priftis K, Umiltà C. Brain damage: neglect disrupts the mental number line. *Nature* 417: 138–139, 2002.